Contribution of gravity waves to the lower thermospheric winter-to-summer meridional circulation in high-resolution WACCM-X

Dai Koshin, Nicholas Pedatella, Anne Smith, and Han-Li Liu (NSF NCAR)

30th annual CESM Workshop: WAWG, June 11, 2025

This material is based upon work supported by the National Center for Atmospheric Research, which is a major facility sponsored by the National Science Foundation under Cooperative Agreement No. 1852977.

Introduction: meridional circulation in the MLT region

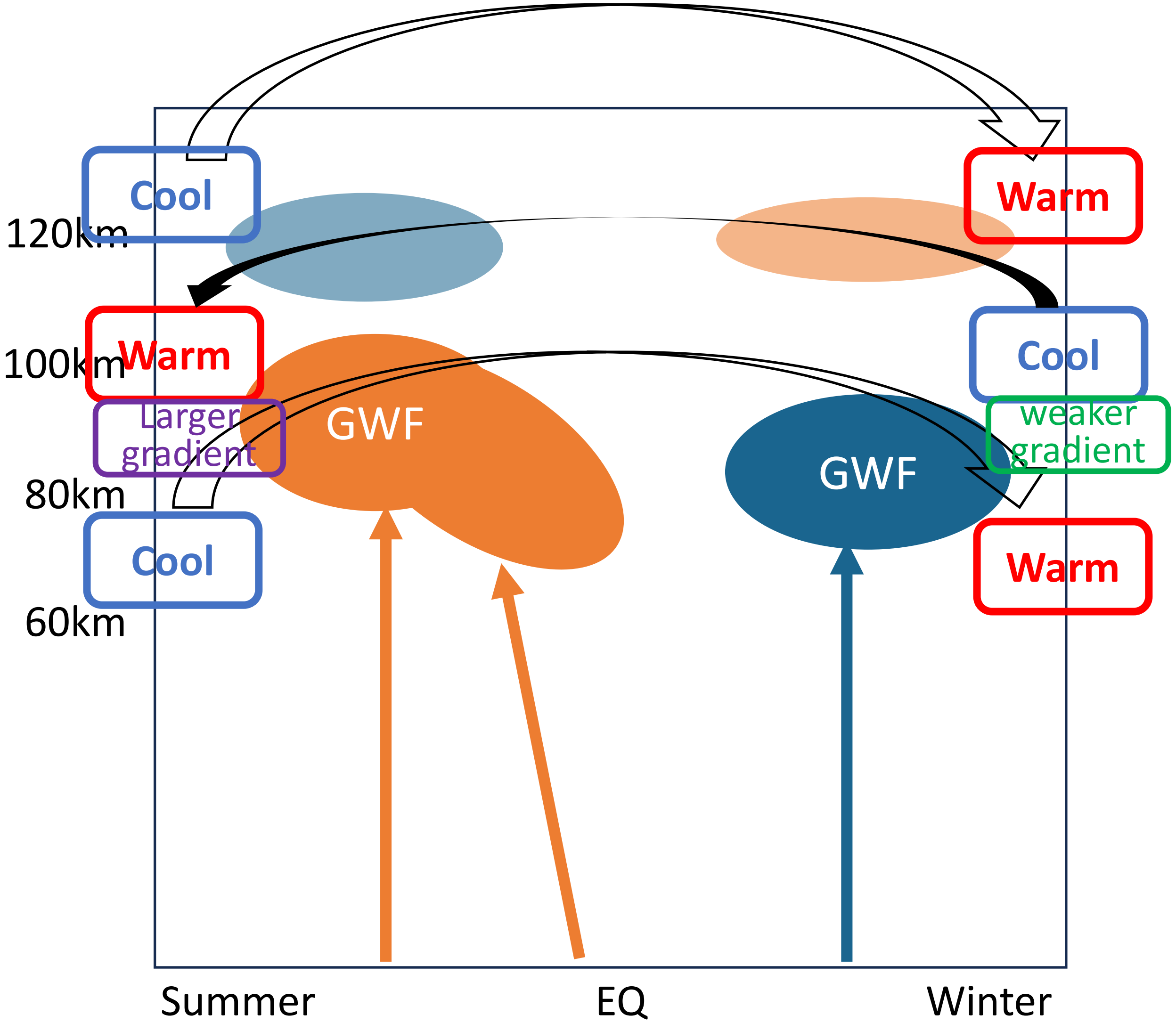

Orange: eastward waves/forcing
Blue: westward waves/forcing

<u>Upper mesosphere</u>: summer to winter

- Gravity wave forcing

<u>Lower thermosphere</u>: winter to summer

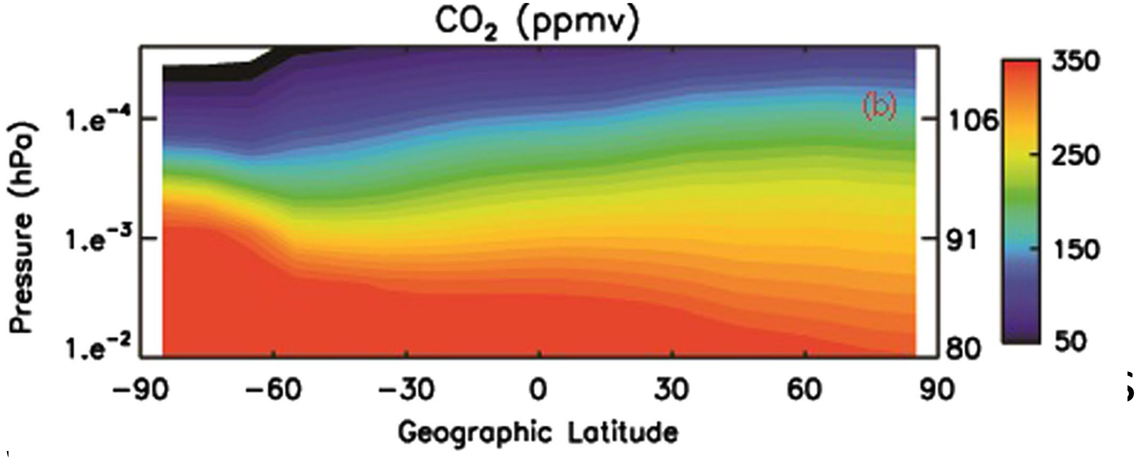

SD-WACCM (2003–2014 Jan; Qian et al., 2017)

- There are several tracer distribution analysis (CO_2, H_2O, NO, O, O/N_2).

<u>Middle thermosphere</u>: summer to winter

- Ion drag, diabatic heating, pressure gradient

Methodology

To analyze the origin and nature of the waves driving the lower thermospheric circulation, the dynamical process through the middle atmosphere is examined.

High-resolution WACCM-X (Liu et al., 2024a; 2024b; 2025)

- Horizontal resolution: **~25 km** (NE120; quarter-degree)
- Vertical resolution: **~0.7 km** (0.1 scale height; 273 levels)
- One-year free-run: 13 January to 31 December
- Small-scale disturbances: waves with $\lambda_x <$ **2000 km**

No gravity wave parameterization

> 20TB

Result

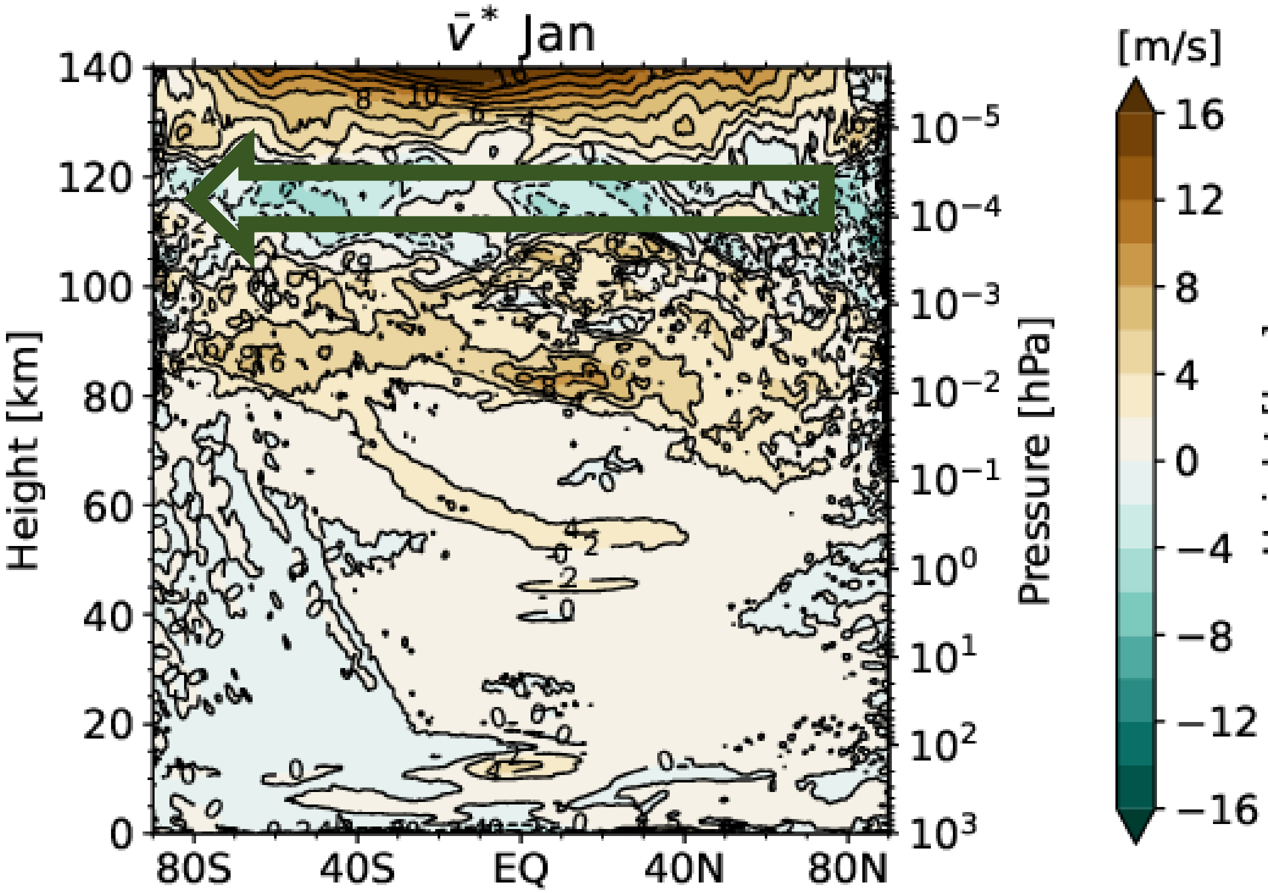

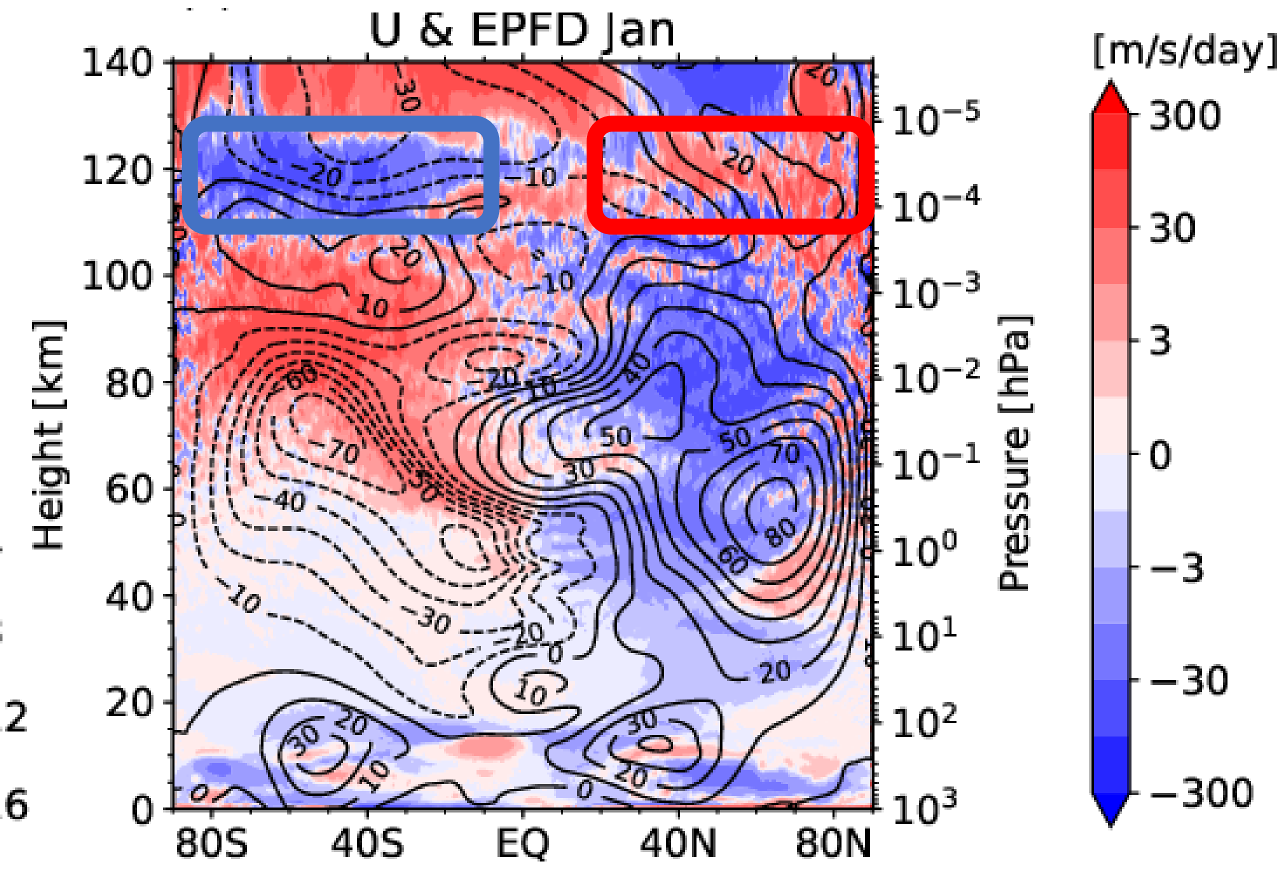

- $\bar{v}^*$: southward flow at z = 110–120 km
- $\nabla \cdot \mathbf{F}$: positive (eastward forcing) in the NH, negative (westward forcing) in the SH

➞ Wave-driven mechanism is considered.

Contribution of small-scale waves

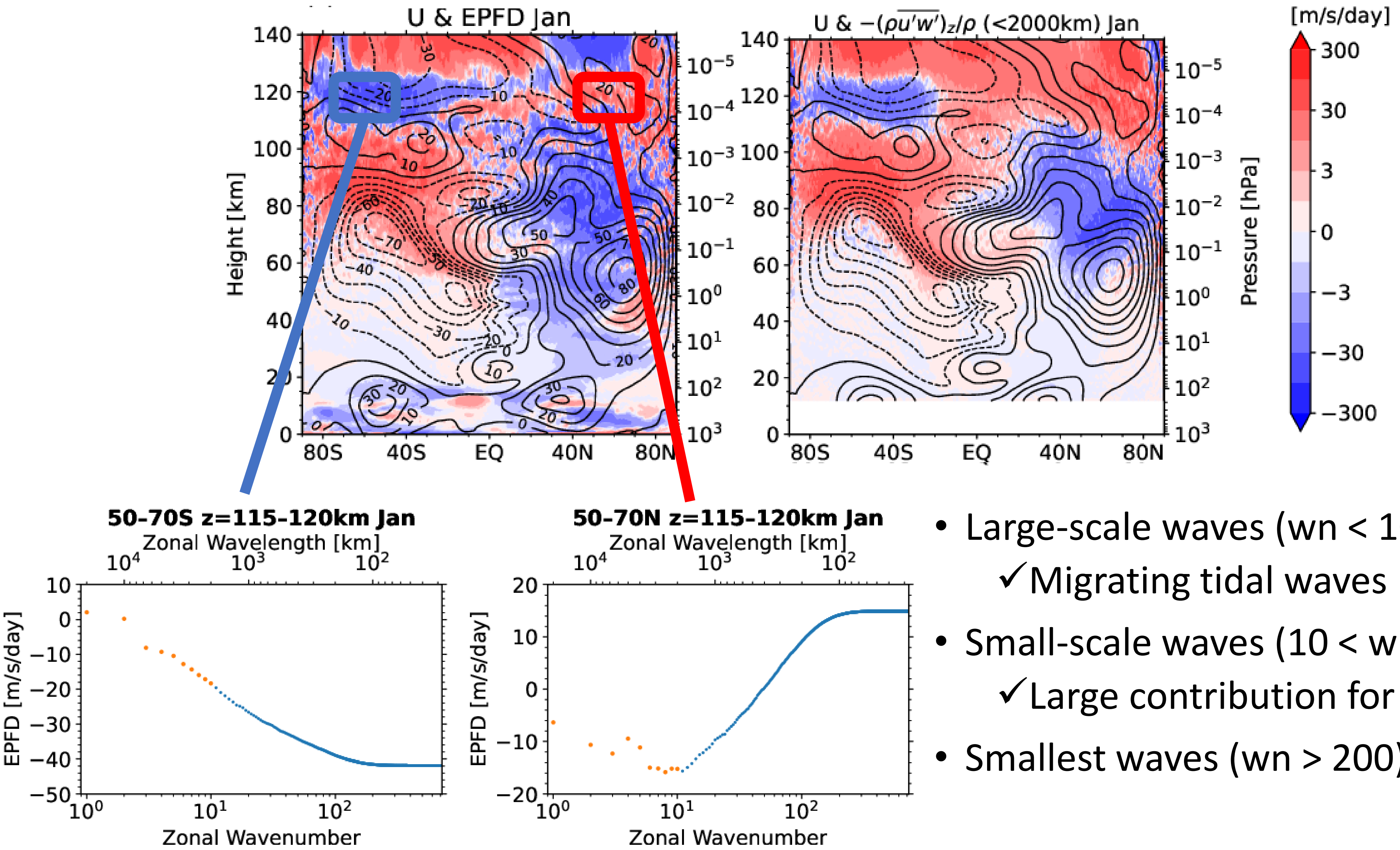

- Large-scale waves (wn < 10): negative
  - ✓Migrating tidal waves
- Small-scale waves (10 < wn < 200)
  - ✓Large contribution for the net forcing
- Smallest waves (wn > 200): negligible

Seasonal variation

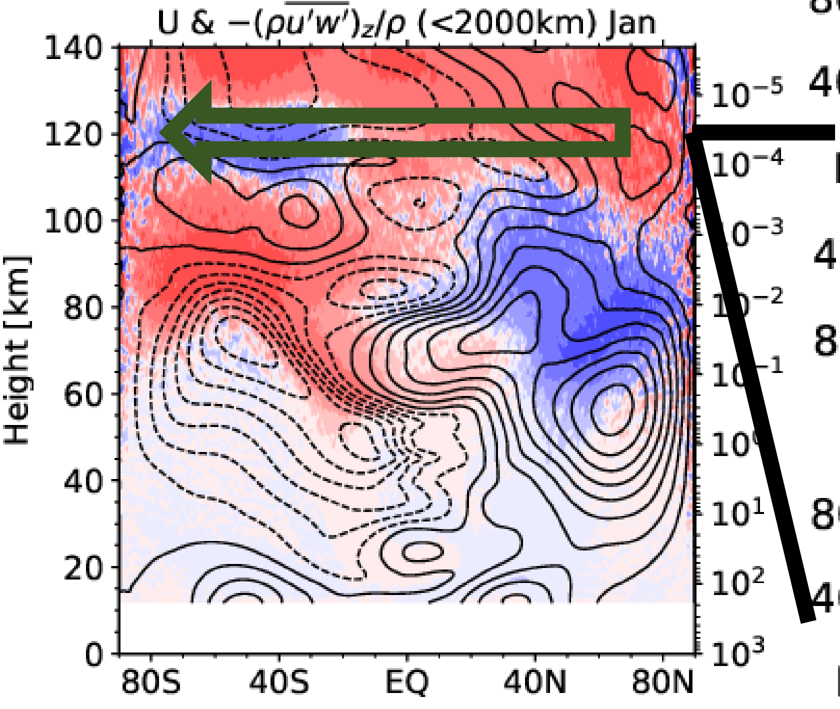

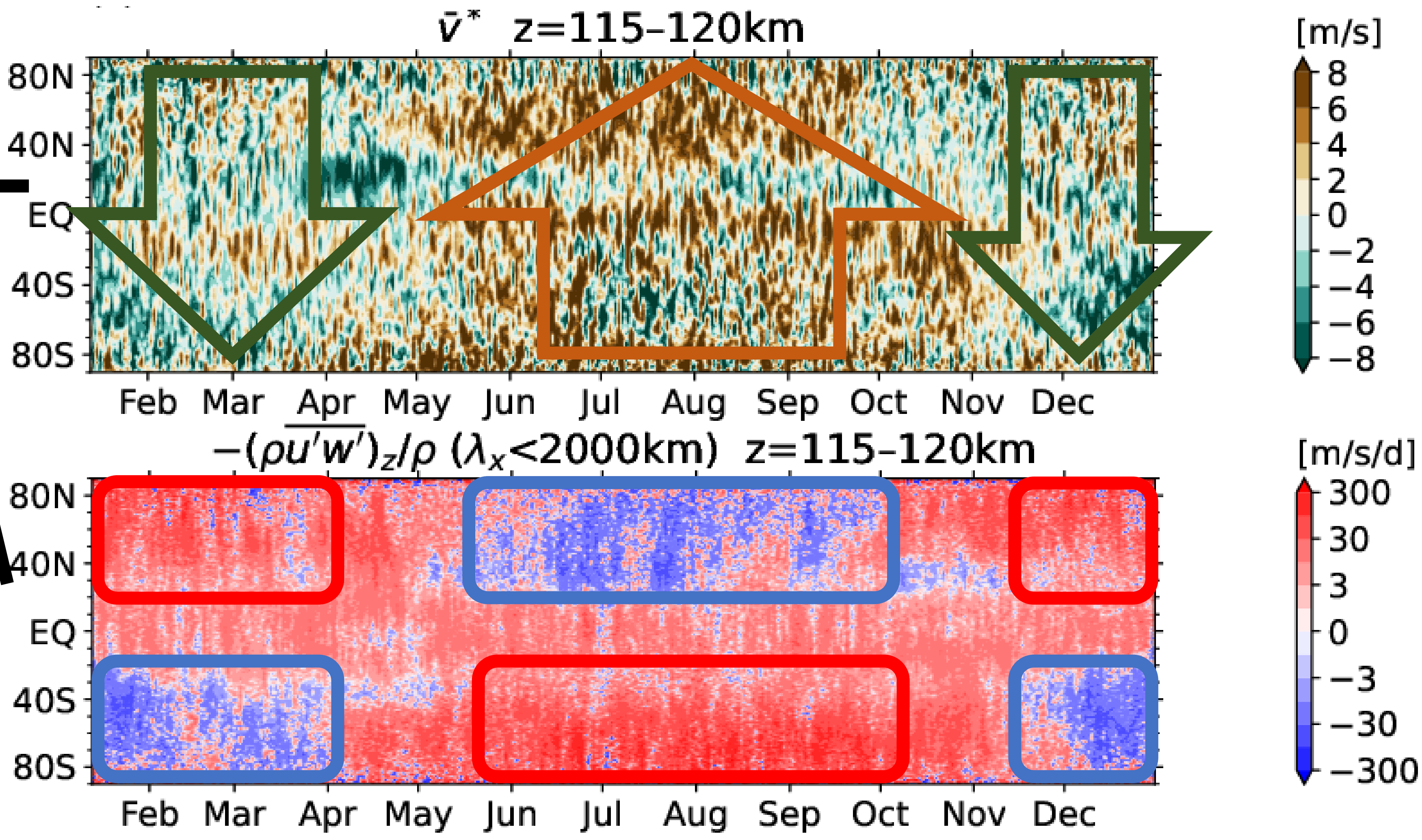

Circulation	Southward (Jan–Mar, Nov–Dec)	Northward (May–Sep)
NH	Positive forcing	Negative forcing
SH	Negative forcing	Positive forcing

Phase speed decomposition

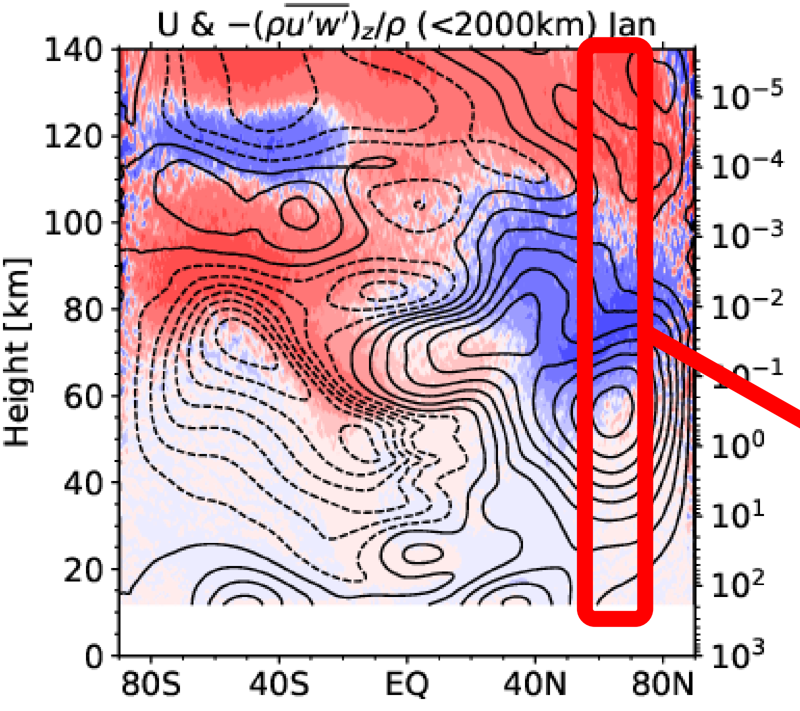

Momentum flux as a function of the phase speed

1. 2D-FFT (x,t) for u and w at each latitude and altitude
2. Cospectrum: momentum flux at each wavenumber & frequency
3. Accumulate the flux along the same phase speed (10 m/s bin)

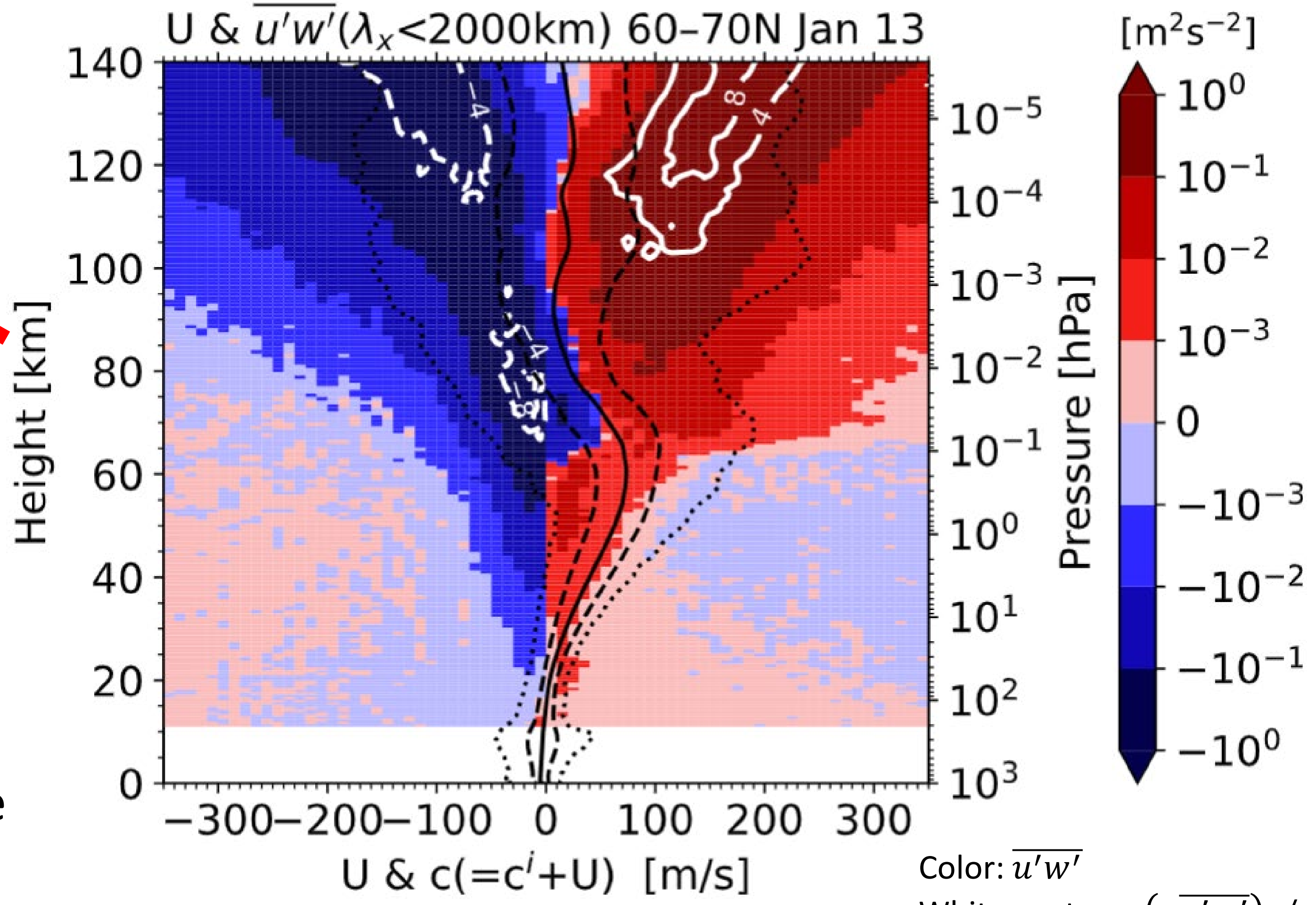

- $\overline{u'w'}$>0 for eastward waves and $\overline{u'w'}$<0 for westward waves ➡ Upward propagation
- Slow westward waves (-30 < c < 0 m/s):
  - ✓Dissipation at z = 65–90 km
- Eastward waves (50 < c <170 m/s):
  - ✓Large forcing in the lower thermosphere
  - ✓Waves slower than U is also dominant, which cannot propagate from below.

Color: $\overline{u'w'}$

White contour: $(\rho\overline{u'w'})_z/\rho$

Black curves: U

Discussion: wave generation

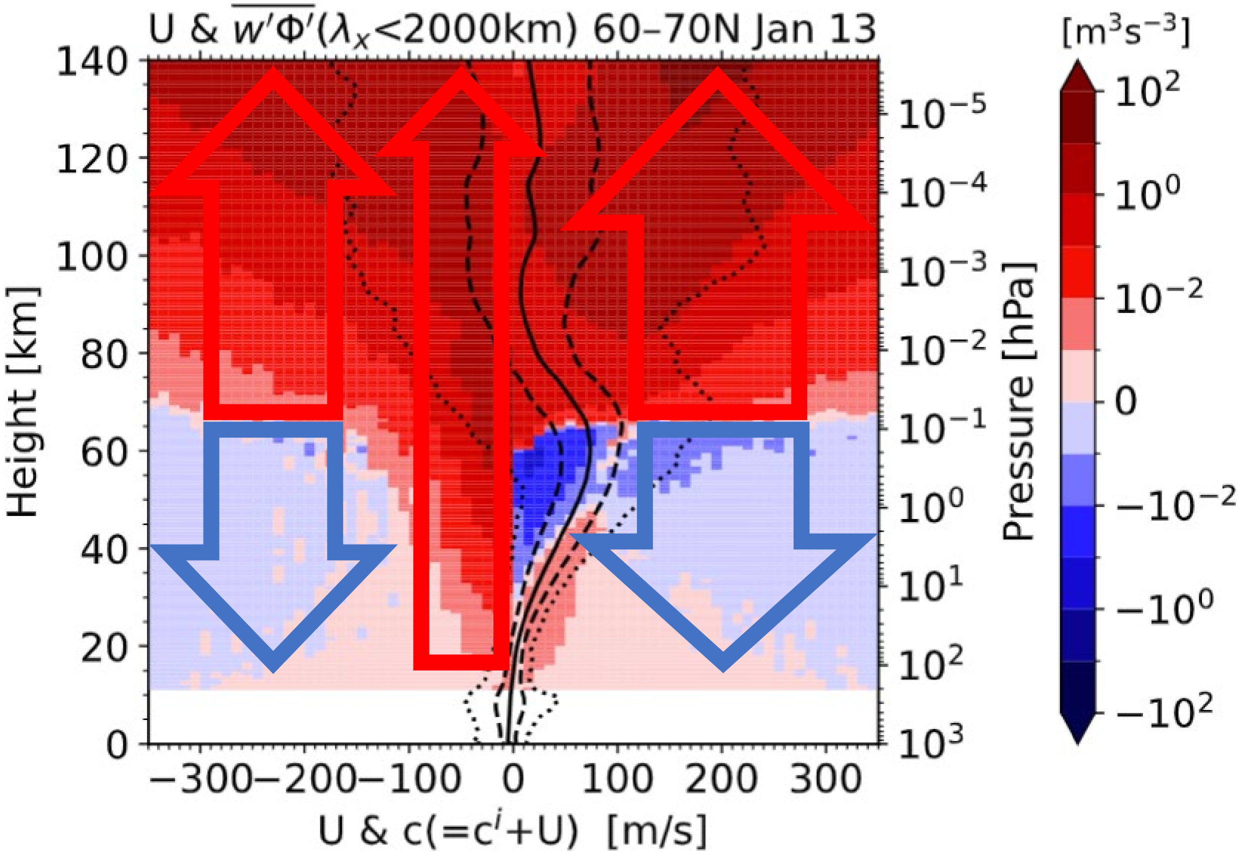

Vertical energy flux due to pressure work ($\overline{w'\Phi'}$): proportional to the vertical wave propagation

- A contrast at z = 67 km: Divergence of eastward waves (c > 0 m/s) and fast westward waves (c < -150 m/s)
- Slower westward waves (-150 < c <0 m/s) are more propagated from the stratosphere.

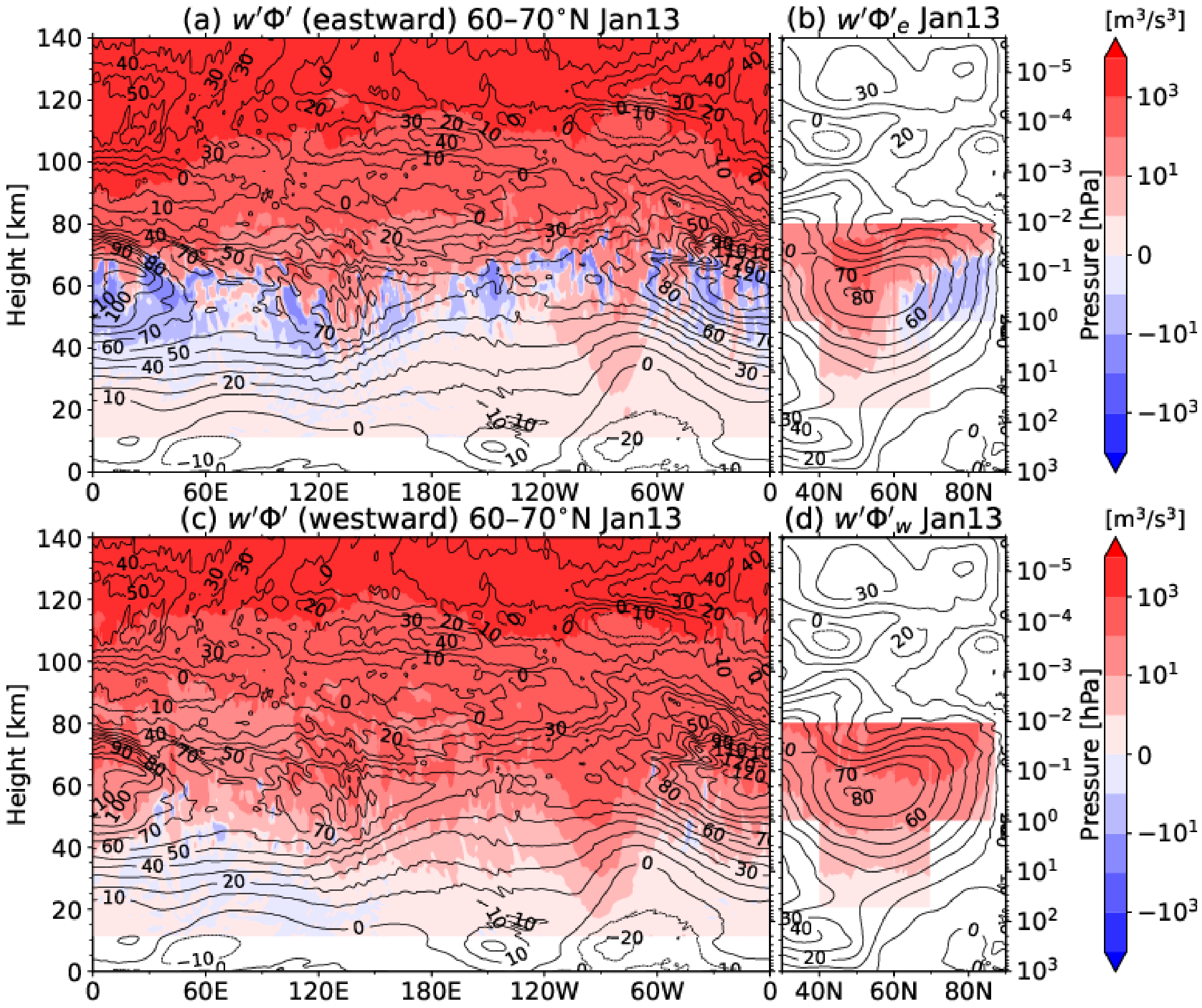

Horizontal distribution of $\overline{w'\Phi'}$:

- Eastward wave divergence is observed above the zonal wind maximum, over wide longitudes and latitudes.
- Is it possible to estimate the wave generation from the mesospheric jet structure?

Discussion: GW generation diagnosis

Absolute horizontal temperature gradient

1. Coarser grid average (2.5°x2.5°: medium-scale background)
2. $|\nabla T| = \sqrt{\left(\frac{\partial T}{\partial x}\right)^2 + \left(\frac{\partial T}{\partial y}\right)^2}$

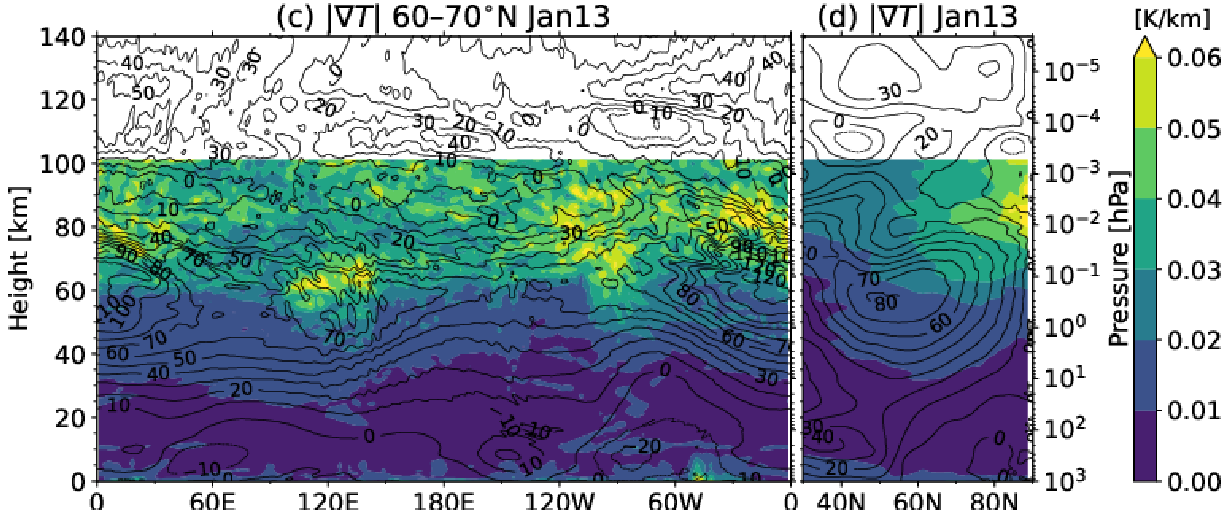

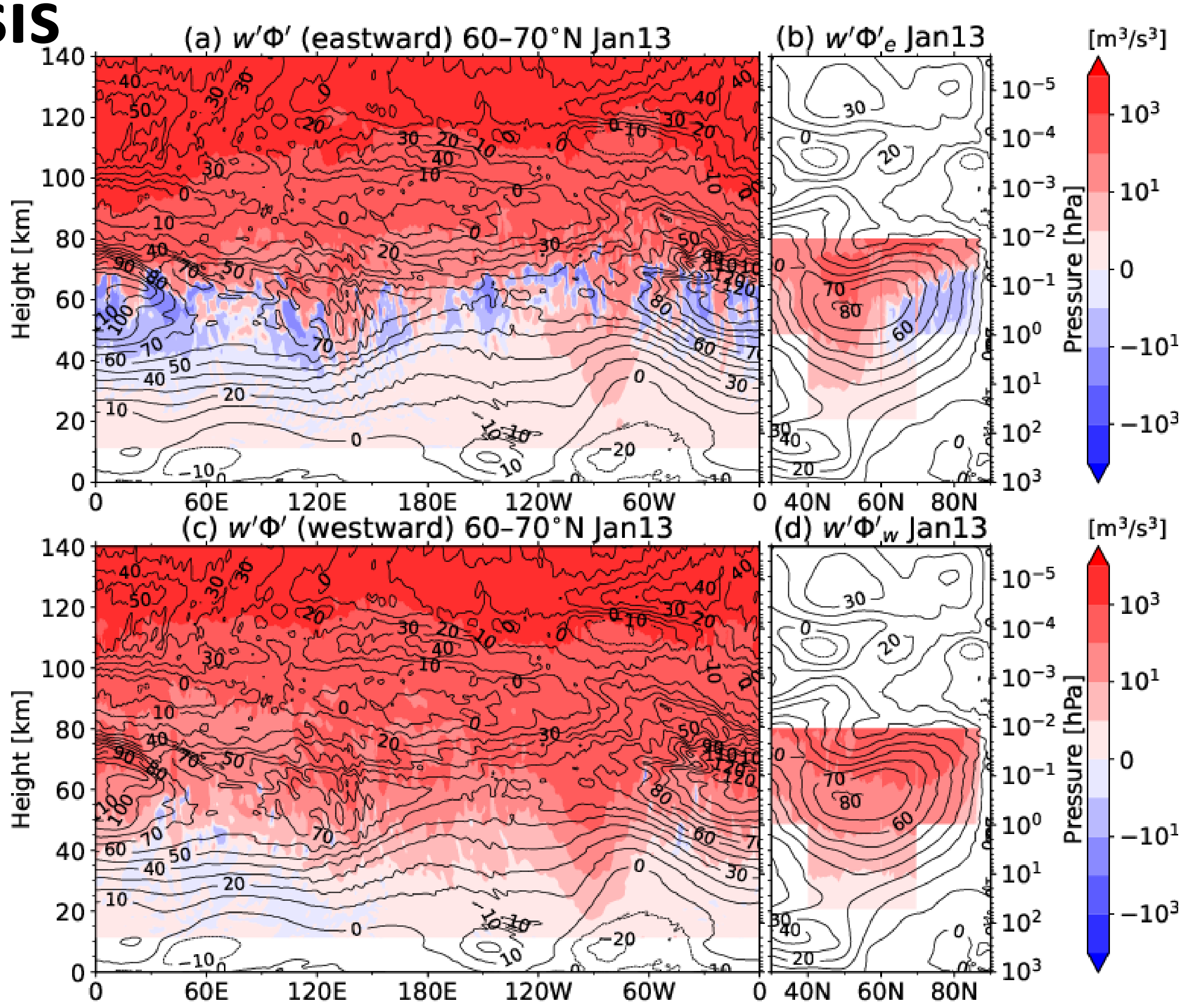

- $|\nabla T|$ generally increases with altitude.
- A large value is observed above the zonal wind maximum.
- The zonal variation is associated with the jet structure (strong zonal wind).

Indicating the wave generation?

Discussion: seasonal variation of wave generation pattern

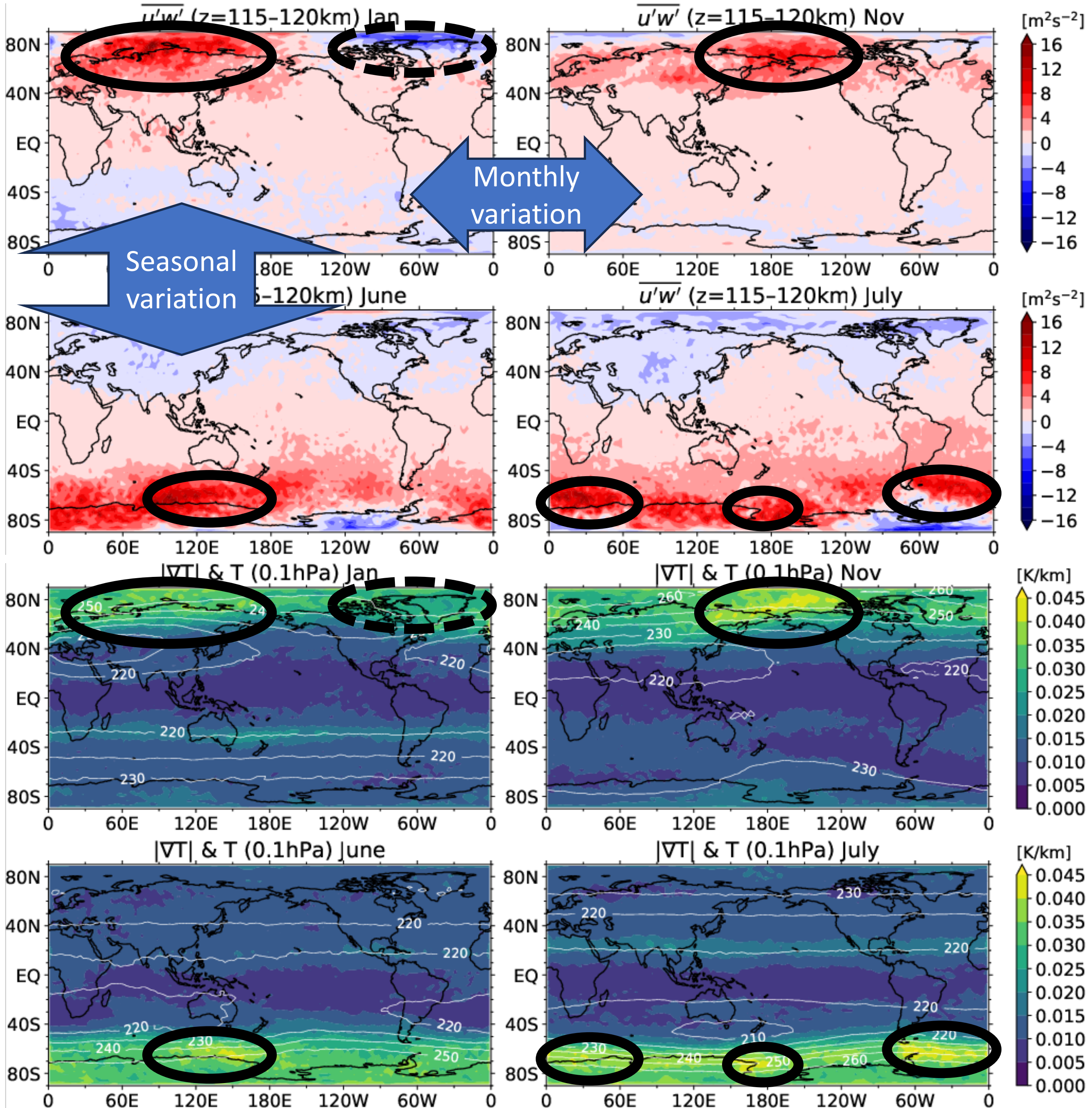

<u>Seasonal variation</u>

- Large positive $\overline{u'w'}$ in the winter high latitudes in the **lower thermosphere**
- Large $|\nabla T|$ in the **winter mesosphere**

<u>Monthly variation</u>

- The distribution of the $\overline{u'w'}$ maximum varies between month.
  - ✓January: Europe to Russia (minimum around Greenland)
  - ✓November: east Russia to Alaska
  - ✓June: 80–180°E
  - ✓July: 0–60°E, 150°E–160°W, 0–80°W
- The pattern of $|\nabla T|$ distribution is similar.

$|\nabla T|$ indicates the wave generation region.

Conclusions

The mechanism driving lower thermospheric meridional circulation is examined.

✓In the winter hemisphere, the generation of eastward gravity waves from the strong westerly jet (polar vortex) is important.

✓Different features for westward waves

- Propagate from lower heights
- Dissipate in the upper mesosphere (➞ Upper mesospheric circulation)

✓Gravity wave generation in the mesosphere could be estimated from the temperature gradient.

↪ Improvement of the parameterization? (analogy to the frontal GW in WACCM)

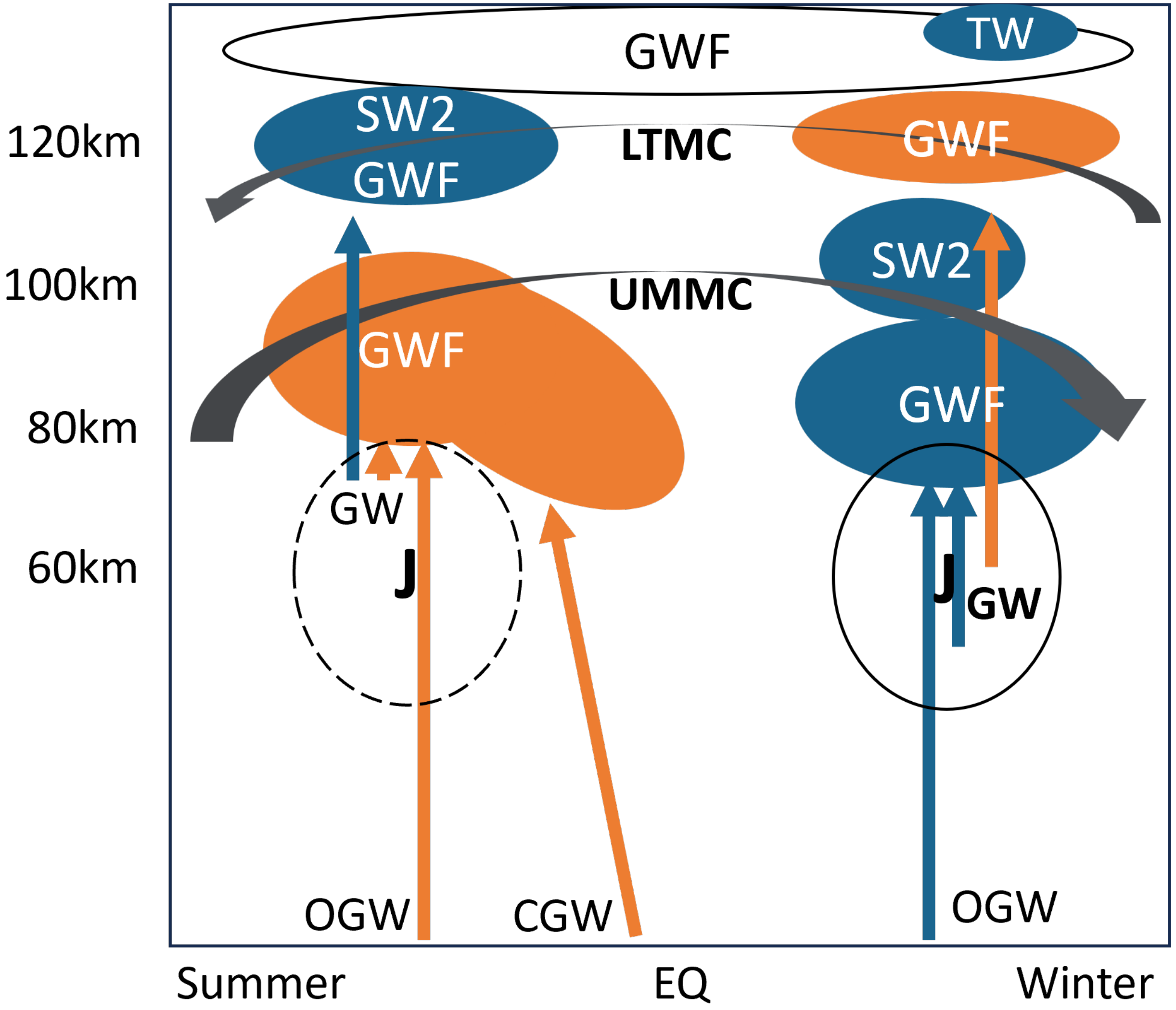

Orange: eastward waves/forcing
Blue: westward waves/forcing

Supplementaly

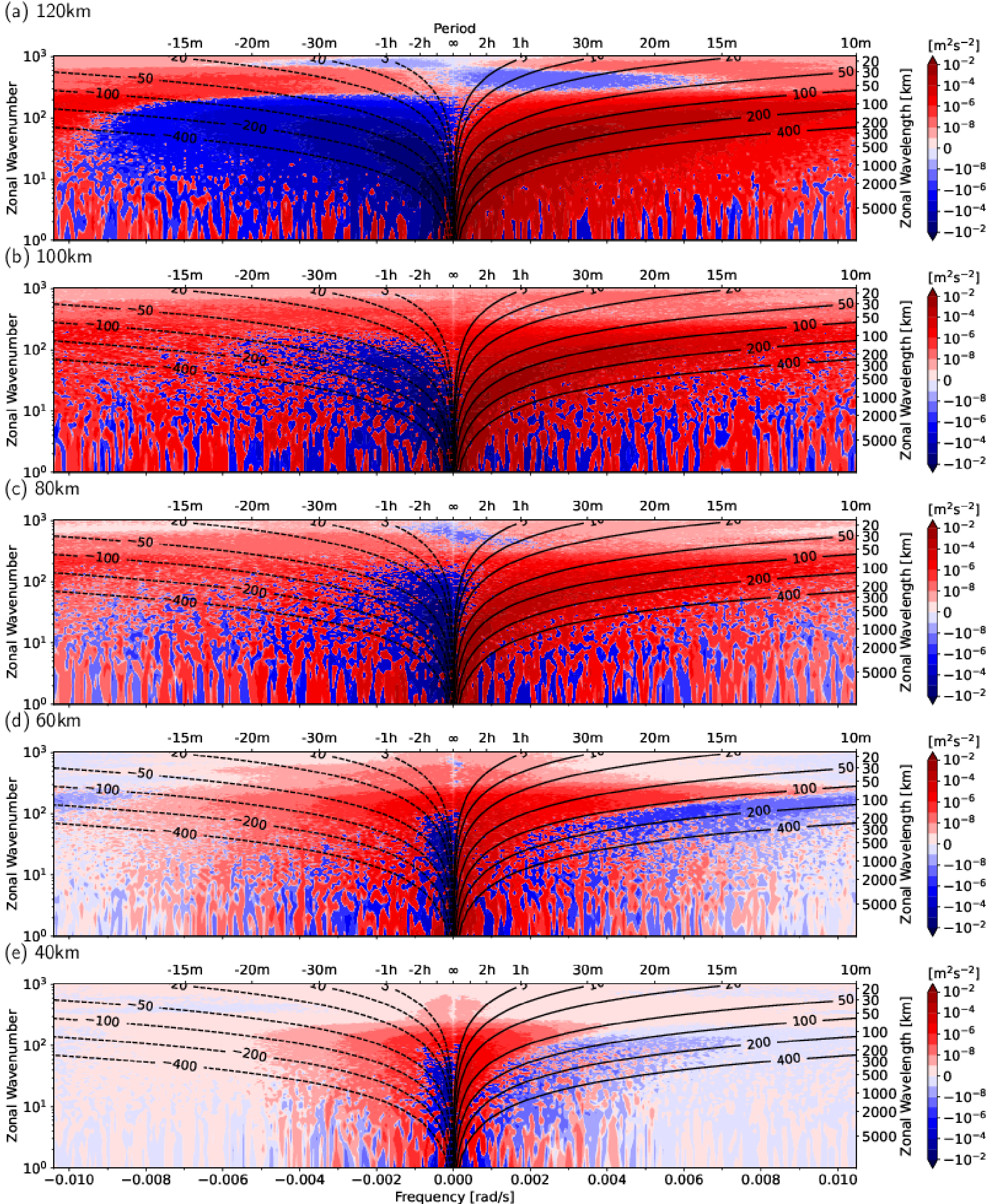
(a) 120km
(b) 100km
(c) 80km
(d) 60km
(e) 40km
Period
Zonal Wavenumber
Zonal Wavelength [km]
Frequency [rad/s]
[m²s⁻²]

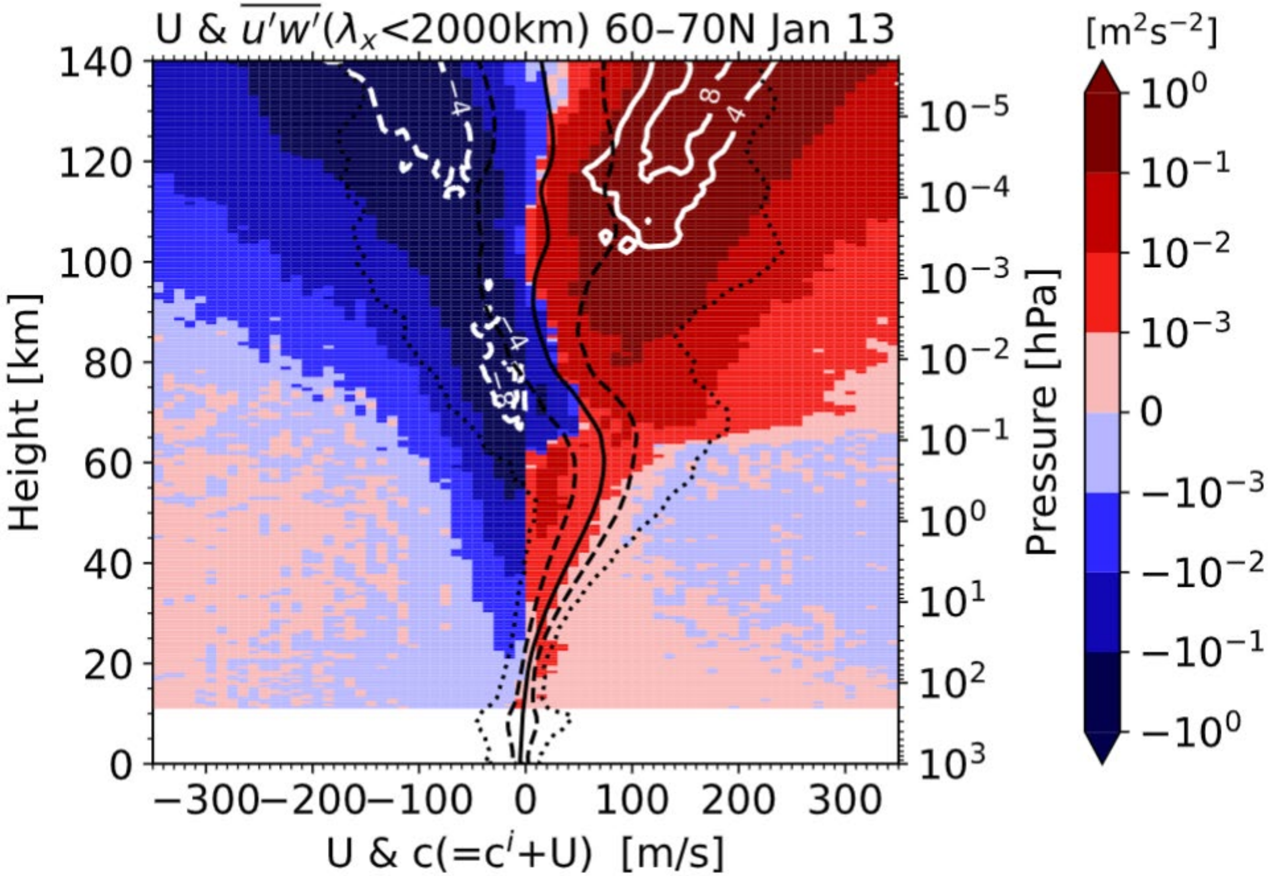
U & $\overline{u'w'}$(λ_x<2000km) 60–70N Jan 13
Height [km]
Pressure [hPa]
U & c(=c^i+U) [m/s]
[m²s⁻²]

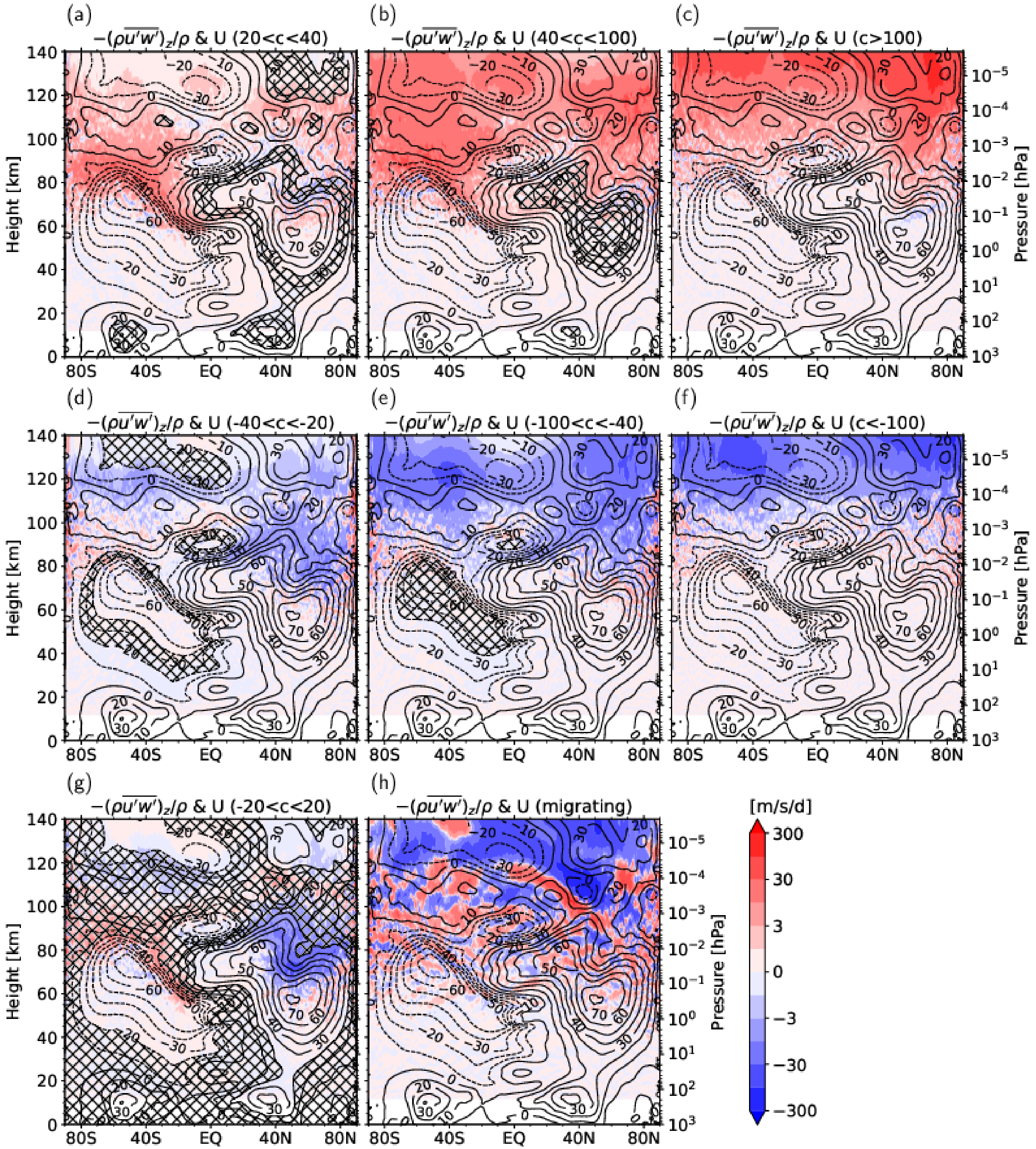
(a)
$-(\rho\overline{u'w'})_z/\rho$ & U (20<c<40)
(b)
$-(\rho\overline{u'w'})_z/\rho$ & U (40<c<100)
(c)
$-(\rho\overline{u'w'})_z/\rho$ & U (c>100)
(d)
$-(\rho\overline{u'w'})_z/\rho$ & U (-40<c<-20)
(e)
$-(\rho\overline{u'w'})_z/\rho$ & U (-100<c<-40)
(f)
$-(\rho\overline{u'w'})_z/\rho$ & U (c<-100)
(g)
$-(\rho\overline{u'w'})_z/\rho$ & U (-20<c<20)
(h)
$-(\rho\overline{u'w'})_z/\rho$ & U (migrating)
Height [km]
Pressure [hPa]
80S
40S
EQ
40N
80N
[m/s/d]
300
30
3
0
−3
−30
−300

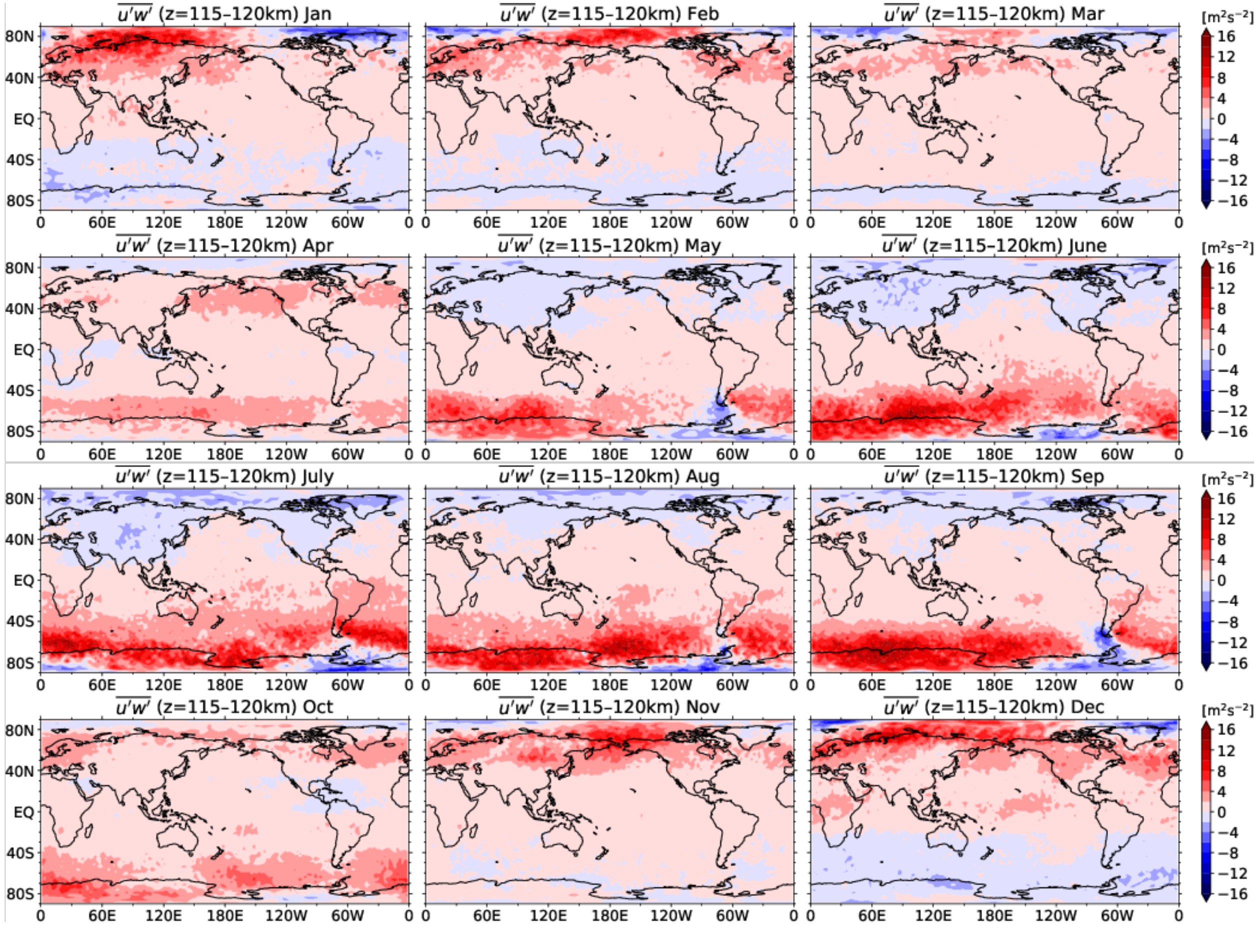

u'w' (z=115-120km) Jan
u'w' (z=115-120km) Feb
u'w' (z=115-120km) Mar
u'w' (z=115-120km) Apr
u'w' (z=115-120km) May
u'w' (z=115-120km) June
u'w' (z=115-120km) July
u'w' (z=115-120km) Aug
u'w' (z=115-120km) Sep
u'w' (z=115-120km) Oct
u'w' (z=115-120km) Nov
u'w' (z=115-120km) Dec
[m²s⁻²]

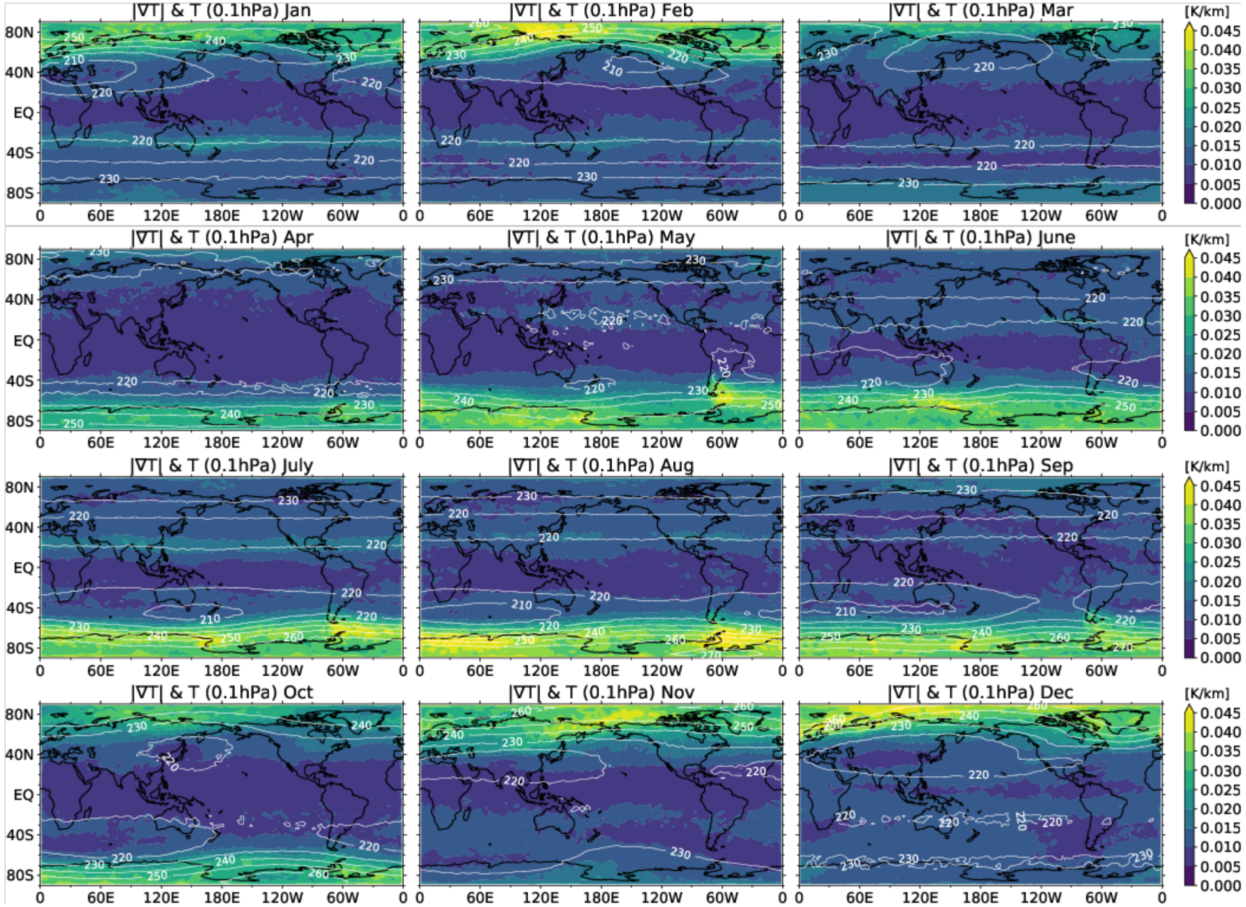

|∇T| & T (0.1hPa) Jan
|∇T| & T (0.1hPa) Feb
|∇T| & T (0.1hPa) Mar
|∇T| & T (0.1hPa) Apr
|∇T| & T (0.1hPa) May
|∇T| & T (0.1hPa) June
|∇T| & T (0.1hPa) July
|∇T| & T (0.1hPa) Aug
|∇T| & T (0.1hPa) Sep
|∇T| & T (0.1hPa) Oct
|∇T| & T (0.1hPa) Nov
|∇T| & T (0.1hPa) Dec
[K/km]

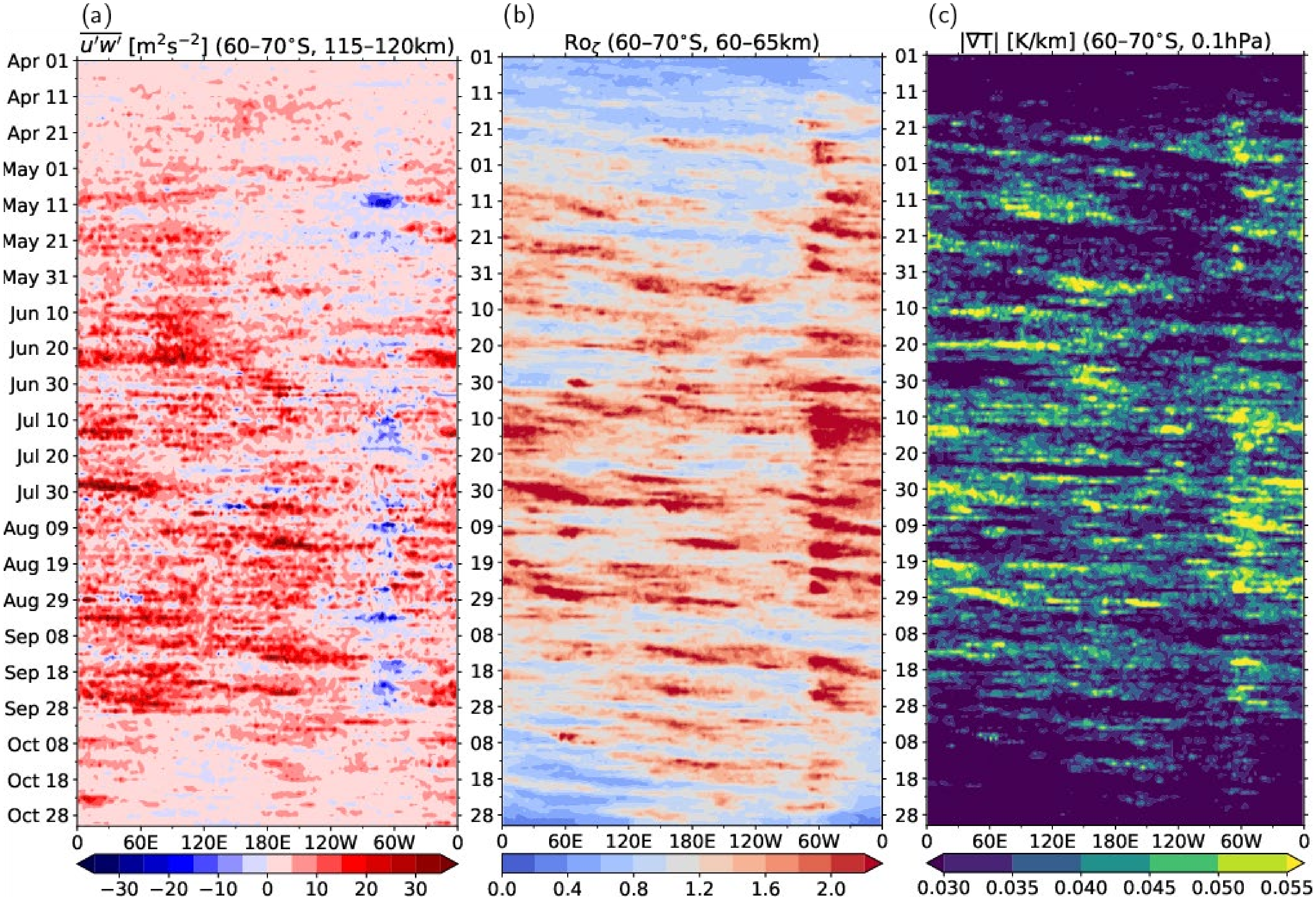
(a)
$\overline{u'w'}$ [m^2s^{-2}] (60–70°S, 115–120km)
Apr 01
Apr 11
Apr 21
May 01
May 11
May 21
May 31
Jun 10
Jun 20
Jun 30
Jul 10
Jul 20
Jul 30
Aug 09
Aug 19
Aug 29
Sep 08
Sep 18
Sep 28
Oct 08
Oct 18
Oct 28
0 60E 120E 180E 120W 60W 0
−30 −20 −10 0 10 20 30
(b)
Ro_ζ (60–70°S, 60–65km)
01 11 21 01 11 21 31 10 20 30 10 20 30 09 19 29 08 18 28 08 18 28
0 60E 120E 180E 120W 60W 0
0.0 0.4 0.8 1.2 1.6 2.0
(c)
$|\nabla T|$ [K/km] (60–70°S, 0.1hPa)
01 11 21 01 11 21 31 10 20 30 10 20 30 09 19 29 08 18 28 08 18 28
0 60E 120E 180E 120W 60W 0
0.030 0.035 0.040 0.045 0.050 0.055